

## FEATURE ARTICLE

## Femtodynamics Reflected in Nanoseconds: Bimolecular Free Electron Transfer in Nonpolar Media

Ortwin Brede\*<sup>†</sup> and Sergej Naumov<sup>‡</sup>

Interdisciplinary Group Time-Resolved Spectroscopy, University of Leipzig, Permoserstrasse 15, 04303 Leipzig, Germany, and Leibniz Institute for Surface Modification, Permoserstrasse 15, 04303 Leipzig, Germany

Received: June 6, 2006; In Final Form: July 13, 2006

The (free) electron transfer (FET) from electron donor molecules to parent solvent radical cations of alkanes and alkyl chlorides exhibits mechanistic peculiarities that are conditioned by the low polarity of these solvents. Because of the negligible solvation of ions in such systems and the almost complete lack of an activation barrier, the electron jump takes place at the very first encounter of the reactants and, as such, in extremely short times of  $\leq 10^{-15}$  s. Molecular oscillations (deformation, bending) occurring within the femtosecond time domain result directly in significant changes of the  $\pi$ - or n-electron distribution in the HOMO ground state of the donor molecule, thereby generating a distribution of conformers. This is considered to be a rationale for a possible generation of different product radical cations in the free electron transfer, which exhibit different spin and charge distribution and, consequently different stability. Experimentally, the latter has been verified for aromatic donors, substituted with mobile, i.e., not rigidly fixed heteroatom-centered groups (various phenol type compounds, thiophenols, aromatic amines, benzyltrimethylsilanes etc.). The individually characteristic product distribution could be visualized and quantified by time-resolved spectroscopy in the nanosecond time domain. On the basis of a manifold of experimental data and supported by quantum-chemical calculations, the free electron transfer phenomenon is analyzed and discussed in detail in this summarizing report. The results presented here stand also for a, seemingly paradox, situation in which the products of a diffusion-controlled bimolecular reaction are governed by femtosecond events.

## 1. Introduction

In the kinetic treatment of bimolecular reactions, intramolecular oscillations of the reactants are usually ignored.<sup>1,2</sup> Among the main features of those processes only the transport by molecular diffusion and equilibrium kinetics are commonly considered. This is symbolized by a formalism displayed in the sequence of equilibria (1), for the example of an ion–molecule reaction.



In contrast, femtochemistry<sup>3</sup> covers local chemical transformations (of single molecules, complexes or other local entities),<sup>4,5</sup> which are tightly controlled by molecular dynamics. Intramolecular dynamic motions occurring in this time range are vibrations, stretching and various other types of deformation modes (bending: torsion, wagging, ...).<sup>6</sup> This means that during these motions bond lengths remain more or less the same, although the angles between atoms or molecular groups may change considerably.

Within aromatic molecules with larger substituents these groups are dynamically twisted against the aromatic ring, with frequencies  $\leq 10^{13}$  Hz at room temperature. Knowledge about these motions originates from infrared and microwave spectroscopy, ultrashort time resolution experiments, as well as from quantum chemical analysis.<sup>7–10</sup>

It is obvious that the deformation motions in the ground state (bending motions, here treated as rotation) affect the electron density distribution within the molecule. This is demonstrated for the singlet state of the thiophenol molecule where the HOMO electrons are distributed in dependence on the angle of twist of the thiol group vs the aromatic ring; see Figure 1.<sup>11</sup> The results have been obtained by density functional theory (DFT) quantum chemical calculations.

As a consequence, for the dynamic case where the rotation (deformation, bending) barrier is not too high ( $E_a \leq 20$  kJ mol<sup>-1</sup>), all these apparently resonant (i.e., uniform) molecules constitute, in fact, a *diversity of molecules*, differing by the angle of rotation (deformation) of the substituent. So, in reality dynamic mixtures exist of identically structured molecules with, however, different electron distributions. In a broader sense we are dealing with a *diversity of (rotational) conformers*.<sup>12,13</sup>

The interesting question, at this point, is if, and to what extent, this diversity of rotational conformers, and thus electronically

\* Corresponding author. E-mail: brede@mpgag.uni-leipzig.de.

<sup>†</sup> University of Leipzig.

<sup>‡</sup> Leibniz Institute for Surface Modification.



Ortwin Brede received his Diploma in Chemistry from the University of Leipzig in 1966. For his Ph.D. he attended the group of Professor Ernst Schmitz at the Institute of Organic Chemistry, German Academy of Sciences, and defended the degree at Humboldt University in Berlin in 1969. Then he worked as a scientist in the Central Institute of Isotope and Radiation Research, Academy of Sciences, Leipzig. Teaching at the University of Leipzig, in 1984 he got DSc title (now habilitation). Five years supported by the Max Planck Society, since 1992 he heads the Interdisciplinary Group Time-Resolved Spectroscopy at the University of Leipzig. In 1993 he became Professor of Physical Chemistry. Applying electron pulse radiolysis and laser flash photolysis, his major interest involves electron transfer processes in nonpolar media, radical chemistry of biological background, and radiation- as well as light-induced primary processes.



Sergej Naumov studied Physics at the Leningrad State University. Supervised by Prof. Treinin, Institute for Optics, he graduated in 1979. Then he was affiliated for about 15 years at the Technical University of Leningrad, teaching Mathematics. Since 1995 he has worked as a senior scientist in the Leibniz Institute of Surface Modification, Leipzig. His scientific interest concerns application of computational chemistry to the interpretation of photo- and radiation-induced elementary reactions, in particular to metatheses polymerization and radical ion chemistry.

different species, possibly manifests itself in distinct and as such identifiable chemical reaction pathways. This may appear as a rather improbable, perhaps even exotic, problem. But here we will report a special type of bimolecular electron transfer, further denoted as “free electron transfer” (FET), which exemplifies, indeed, this situation. It is characterized by an extremely rapid electron jump from the donor molecule (S) to the accepting parent ion derived from a nonpolar solvent (RX = alkane, alkyl chloride).<sup>14–16</sup> The FET gross reaction is generally described by



Applying such an electron transfer to the ionization of phenol (S = C<sub>6</sub>H<sub>5</sub>OH), a surprising observation was made. Instead of

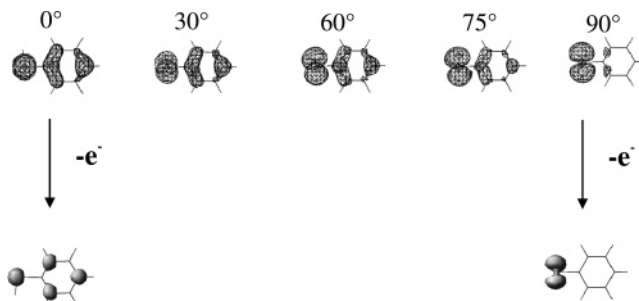
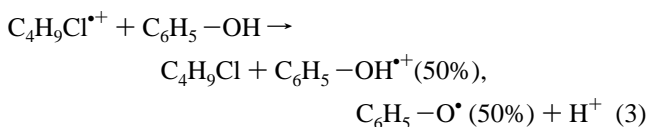


**Figure 1.** Thiophenol: electron density distribution of the HOMO dependent on the angle of twist of the C–S bond (upper part); spin density distribution in the radical cations for the planar and the twisted state (lower part).

the expected phenol radical cations as the exclusive product at the earliest time scale of recording (low ns range), an instant, characteristic 1:1 mixture of phenol radical cations and phenoxy radicals was observed.<sup>14</sup> Reaction 3 shows FET from phenol to

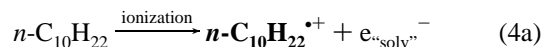


butyl chloride parent ions. Analogous results were obtained in the electron-transfer involving various substituted phenols and other chalkenols.<sup>14,15</sup>

In view of the above considerations, we forwarded those molecular oscillations as rationale for this unexpected result. It is based on the plausible assumption that the actual electron jump happens extremely rapidly, i.e., within  $\leq 1$  fs. In the approach of the reactants in our system (eqs 2/3), this electron jump from the solute molecule to the parent ion would thus happen faster than the deformation motions ( $\geq 100$  fs) of the donor molecule. The rotation-controlled conformer mixture of the donor may thus well be reflected by different products.<sup>14</sup> In the following, this will be discussed in further detail and generalized as a more common phenomenon.

## 2. Parent Ions and Free Electron Transfer in Nonpolar Solutions

For decades it has been known that molecular ions derived from alkanes or alkyl chlorides are metastable in liquid, nonpolar surroundings. They can be produced by photoionization,<sup>17</sup> but stationary radiolysis of low-temperature glasses<sup>18–22</sup> and, in particular, time-resolved electron pulse radiolysis<sup>16,23,24</sup> are even easier ways to generate and characterize parent radical cations. At room temperature, the lifetime of the parent radical cations in nonpolar solvents amounts to up to 200 ns, and is dependent on the solvent structure. Equations 4a,c show, as representative



examples, the radiation-induced ionization of *n*-decane<sup>25</sup> and of *n*-butyl chloride.<sup>26</sup> To prevent the inherently rapid neutralization in the radiolysis of alkanes, the highly mobile solvated electron is usually transformed into nonreactive anions, e.g.,

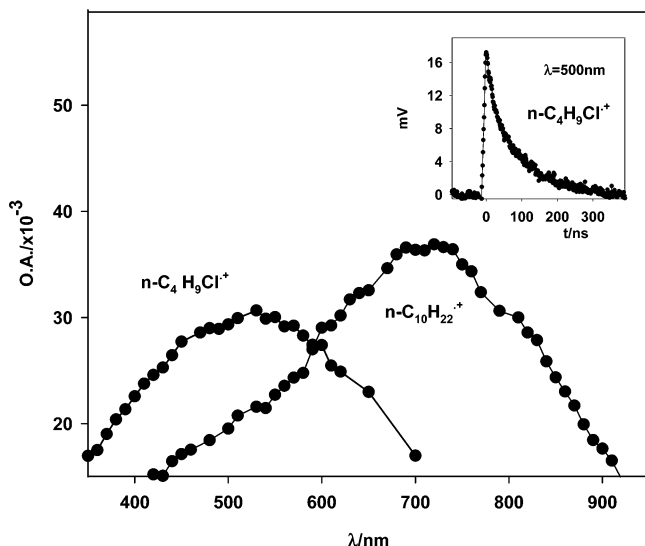


**Figure 2.** Optical absorption spectra of parent radical cations taken in the pulse radiolysis of the pure solvents *n*-decane or *n*-butyl chloride. The inset shows a time profile of the *n*-butyl chloride radical cation at a characteristic wavelength.

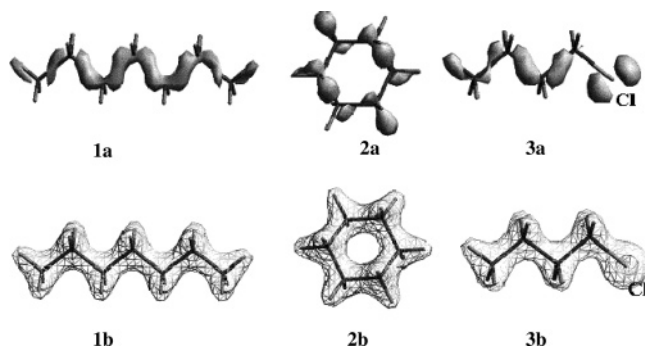
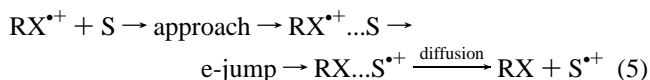


**Figure 3.** Spin density distribution (a, upper part) and charge distribution (b, lower part) of the radical cations derived of *n*-heptane (1), cyclohexane (2) and *n*-butyl chloride (3).

into chloride ions by addition of carbon tetrachloride (reaction 4b) or, in the case of *n*-butyl chloride, by reaction with the solvent.

The thus formed parent radical ions (denoted bold-faced) are well observable in time-resolved optical absorption spectroscopy. This is shown for the chosen examples in Figure 2.<sup>25,26</sup> The spectra exhibit broad bands in the VIS and NIR optical range. A representative time profile is given as an inset.

The radical cations derived from alkanes ( $\text{RH}^+$ ) and alkyl chlorides ( $\text{RCl}^+$ ) represent pure  $\sigma$ -bonded systems. Hence spin and charge density are equally distributed over the whole molecule, which is shown in Figure 3 for some representative examples.<sup>11</sup> From these properties and because of their large ionization potentials,<sup>27</sup> the parent solvent radical cations  $\text{RX}^+$  ( $\text{X} = \text{H}, \text{Cl}$ ) are extremely good electron-transfer oxidants. The entire scavenger reaction sequence (eq 5) can easily be followed by analyzing the time profiles of the solvent radical cations as well as the transient product species.



Within the course of this FET process, the parent radical cation regenerates a solvent molecule and, therefore, becomes anonymous in the solvent surrounding. Instead of the usual quasi-equilibrium situation<sup>28,29</sup> a simple forward process takes

place. The individual steps of it are the diffusional approach and the electron jump. The diffusion part of the products does not make sense in this case and, consequently does not need to be considered. The most remarkable peculiarities of this electron-transfer type are summarized in the following:

- The term free electron transfer (FET)<sup>14,15</sup> has been introduced because the parent ions are only very weakly solvated, if at all. So, in the first approximation any interaction with the solvent molecules can be neglected. In the nanosecond scale, however, the solvent ions are relaxed to the thermal equilibrium.

- The overall reaction 2 was found to be diffusion-controlled; i.e., the rate determining steps are in each case the transport processes such as molecular diffusion (relaxed parent ions)<sup>30,31</sup> or, in special cases, “hopping” (positive holes).<sup>32–35</sup> The latter, incidentally, exhibits rate constants of up to 200 times higher than the diffusion-controlled value for molecular ions. This clearly hints at the general possibility of rapid transport and unhindered electron transfer.

- After the encounter of the reactants, the actual electron jump from the solute to the parent solvent ion is a nonadiabatic process and proceeds at times comparable to that of an unhindered electron flux in molecular entities; i.e., it proceeds in times around 1 fs or faster.<sup>36</sup>

- With such a rapid irreversible electron jump, the FET should not follow defined equilibrium kinetics, not pass through a classical encounter complex and, as a consequence of all this, render the parent ion anonymous after the electron jump.

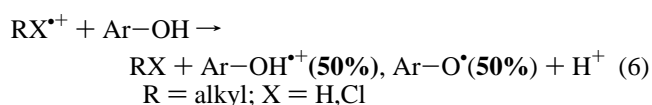
- The rationales for the extremely rapid electron transfer are the uniform charge (spin) distribution in the solvent parent ions, the high free energy of the reaction, and the overall influence of the nonpolar surroundings.<sup>11</sup>

By comparison with the electron transfer in polar liquids<sup>37</sup> and in gases,<sup>38</sup> the FET kinetics in nonpolar liquids tend more toward those of the gas phase (collision kinetics). Influences due to the heat bath condition in the condensed phase, and the rapid thermalization and relaxation of the species have to be taken into account, of course. The above listed properties of the free electron transfer<sup>11</sup> were derived from a thorough analysis of the products from the scavenger side, as described below in detail.

### 3. Unusual Product Distribution in FET

Despite the limited lifetime of the solvent radical cations ( $\tau < 200$  ns) and the diffusion controlled rate for the overall bimolecular process, the electron transfer from any solute ( $c \leq 10^{-2}$  mol dm<sup>-1</sup>) to the solvent parent ions (cf. reaction 5) can be observed exclusively and without ambiguity in pulse radiolysis experiments.<sup>39</sup> That is because any other transients (radicals, carbenium ions etc.) are much less reactive than the solvent parent ions. Consequently, also the products of the electron transfer (5), namely, the radical cations of the electron donor, are directly observable, at least in most cases.

As mentioned already briefly, a parallel generation of phenol radical cations and of phenoxy radicals, in a 1:1 ratio, has been observed in the oxidation of phenol-type compounds ( $\text{ArOH}$ ),<sup>11,14,15,40,41</sup> reaction 6. This happens independent of the type of the nonpolar solvent ( $\text{RX}$ )<sup>15</sup> or electronic effects caused by further substituents at the aromatic ring.<sup>14</sup>



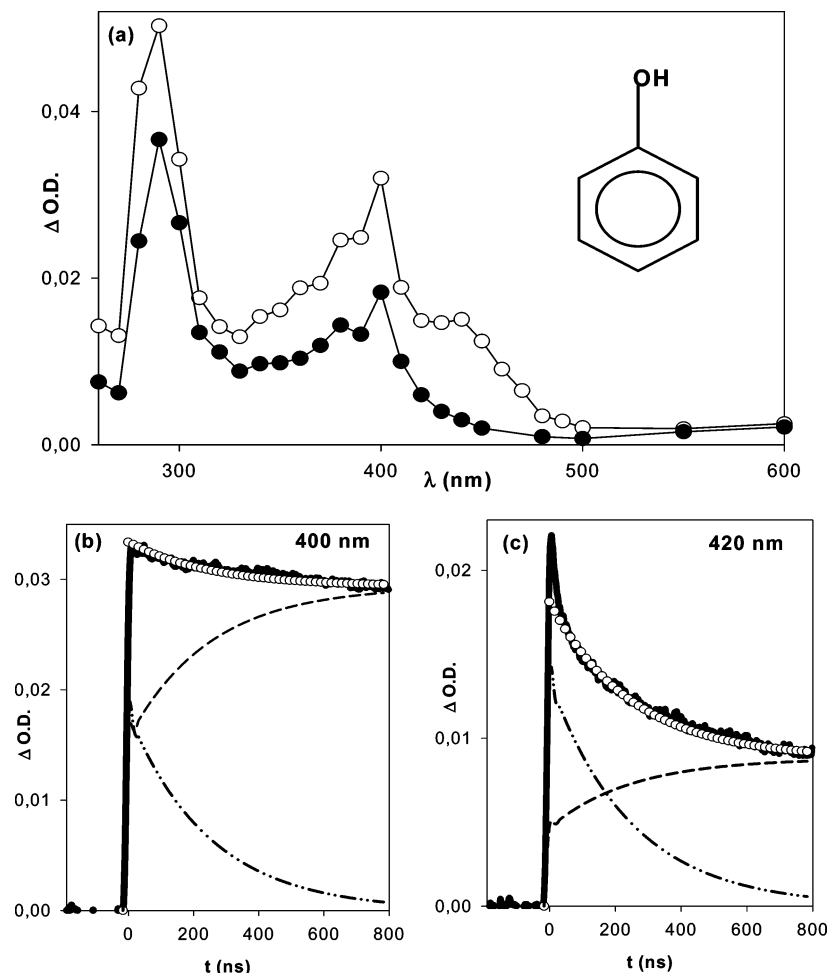


**Figure 4.** Pulse radiolysis of phenol ( $10^{-2}$  mol  $\text{dm}^{-3}$ ) in *n*-butyl chloride: optical absorption spectra taken 30 ns after the pulse (○), and after addition of 0.1 mol ethanol, taken after 1  $\mu\text{s}$  (●). Parts b and c show characteristic time profiles simulated with the assumption of a rapid and delayed formation of  $\text{ArO}^{\bullet}$  by transformation of  $\text{ArOH}^{\bullet+}$  (mechanism in reaction 7a–c).

Figure 4 demonstrates this effect by showing transient absorption spectra taken in the pulse radiolysis of phenol in *n*-butyl chloride solution.<sup>11</sup> The primary solvent radical cation is formed in the course of the 10 ns electron pulse. Reaction 6 then happens within a few tens of nanoseconds. Hence the product spectrum taken 30 ns after the pulse exhibits the typical absorption bands of phenol radical cations ( $\lambda = 420$  nm) and phenoxyl radicals ( $\lambda = 400$  nm). Both species are formed with the rate of the bimolecular electron transfer of  $k_6 = 10^{10}$   $\text{dm}^3 \text{mol}^{-1} \text{s}^{-1}$ . This rate constant has been determined by analyzing the kinetics of the decay of the solvent radical cation.<sup>11</sup> For unambiguous assignment, the phenol radical cation  $\text{ArOH}^{\bullet+}$  was quenched with ethanol or other additives of increasing polarity (see lower spectrum).

The ratio between the product transients was determined by kinetic simulations<sup>11,42</sup> based on the observation that the metastable phenol radical cation eventually decayed within 500 ns under formation of further, i.e., secondary phenoxyl radicals; see reaction 7c. This delayed conversion of the phenol radical cations (7c), observed in the nanosecond range, allows us to calculate the yields and respective ratio of the promptly formed species given in eq 6 (50% phenol radical cations, 50% phenoxyl radicals).

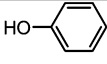
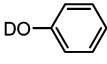
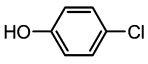
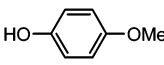
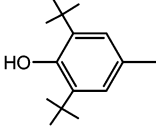
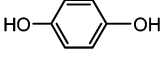
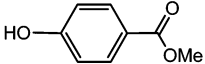
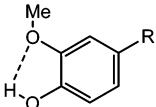
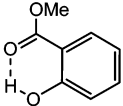
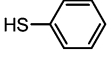
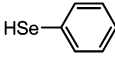
As elucidated in detail later on, similar effects were found using a variety of other electron donors such as differently substituted phenols,<sup>11,14,15</sup> thiophenols,<sup>43</sup> selenophenol,<sup>44</sup> diphenols,<sup>41</sup> naphthols<sup>40</sup> and compounds with combinations of such

hetero substituents.<sup>45</sup> In each case a parallel formation of scavenger radical cations and neutral donor radicals took place, cf. Table 1.

Returning to the former question whether molecular rotation and bending motions can influence the product pattern of bimolecular electron-transfer reactions, it is hypothesized that both products ( $\text{ArOH}^{\bullet+}$ ,  $\text{ArO}^{\bullet}$ ) originate from the free electron transfer involving different (rotation) conformer states of the donor. As has been shown already in Figure 1 for the example of thiophenol, the HOMO electrons shift with increasing angle of rotation from the aromatic ring to the heteroatom. This seems to be true also for all phenols.<sup>11</sup> Here it should be mentioned that the term rotation stands for the complexity of the deformation motions.

The rotation motion around the Ar–C–OH axis generates, as mentioned, a diversity of momentary electron distributions and thus very *mixed conformer states*. This diversity can hardly be introduced into an all-comprising chemical model. Hence, for simplification we define and further consider only two borderline states: the *planar state* stands for the molecules with low angle of twist, whereas the *perpendicular state* includes the molecules with higher deformation angle. This extrapolated simplification appears justified because it describes the product situation, both qualitatively and quantitatively. The important features are that in the planar molecule the electrons are distributed over the whole molecule (in analogy to the picture of resonance of thiols, Figure 1, on the left) and in the perpendicular state electrons

**TABLE 1: Experimentally Obtained Lifetimes  $\tau$  of Chalkogenol Radical Cations in BuCl and the Ratio of the FET Products (ArOH<sup>•+</sup> and ArO<sup>•</sup>) Compared with DFT B3LYP/6-31G(d) Calculated Dynamics Parameters<sup>a</sup>**

Phenol radical cation	exp [ns] BuCl	$t_{\text{bending}}$ [ $10^{-15}$ s]	$t_{\text{valence}}$ [ $10^{-15}$ s]	$E_a$ kJ mol <sup>-1</sup> singlet (cation)	product ratio (•+)/(•)	remarks	ref.
	280	97	9.3	12.6 (62)	50:50		11, 14
	330			12.6	50:50	deuterated phenol	11
	330	98	9.3	13.0 (55)	50:50		11
	330	110	9.3	10.0 (57)	50:50		11
	470	35	9.1	9.8 (46)	50:50	sterically hindered phenol	11
		100	9.3	9.7 (60)	40:60	all biphenols	41
	89	9.3	9.3	17	50:50	para-salicylate	46
	294	12.8	12.8	34 (50)	62:38	curcumin	47
	294	12.8	12.8	61	100:0	ortho-salicylate	46
	294	12.8	12.8	1.7 (89)	35:65	various thiophenols	43, 11
	347	14.8	14.8	2.9 (82)	10:90	selenophenol	44, 11

<sup>a</sup>  $t$  = time of one rotation (bending) or vibration period (valence);  $E_a$  = activation energy of the OH group rotation in the ground state (singlet) and as a radical cation (in brackets);  $T_{\text{exp}}$  = experimentally measured lifetime.

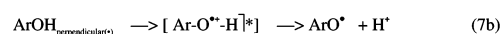
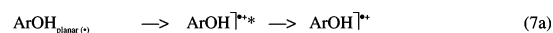
are very localized on the heteroatom (Figure 1, right-hand side). Upon ionization of the molecules in either of these states, the charge and spin distribution should reflect the electron distribution in the ground state. This means that in the very beginning we get two different types of product radical cations, one with charge distributed over the whole molecule, and the other one where the charge is localized at the heteroatom. In the latter the O–H bond is obviously weakened, with the result that this type of phenol radical cation is rather unstable and deprotonates immediately. In fact, appropriate bond energy calculations corroborate this conclusion.

For the example of the FET involving phenols (cf. also reaction 6) we can now put everything into concrete terms, as symbolized by the reaction sequence (7). The rapid deprotonation in reaction 7b is assumed to occur within the first vibrational motion of the corresponding O–H bond.

In our picture concerning the product formation in FET in dependence on the bending motion of the C– $\varphi$ –OH bond, it

should be the activation energy  $E_a$  of the rotational barrier that determines the mobility of the bond. Consequently, the product distribution (assumed conformer ratio) should show a significant dependence on  $E_a$ .

This assumption can be judged by analyzing the data of Table 1. Here, relevant kinetic and dynamic data are compiled for different types of phenols and other chalkogenols. They include times for one vibrational motion (ArO  $\leftrightarrow$  H) and for one



rotational motion (Ar- $\curvearrowright$ -OH), as well as the activation energies of the rotation barrier in singlet and in radical cation state ( $E_a$ ).

Despite the different electronic and structural effects of substituents, the “kinetic” data for the “simple” phenols look quite similar and, perhaps surprisingly, also the ratio of the primary formed phenol transients shows a constant value of 50:50. In all these cases a nonhindered bending oscillation is evident for the ground state and, in fact, the calculated  $E_a$  of bending amounts to less than 15 kJ mol<sup>-1</sup>. This holds also for *meta*- and *para*-salicylate<sup>46</sup> (*meta* data not explicitly listed in Table 1).

In the case of curcumin a weak hydrogen bonding hinders unrestricted rotational motion (five-membered ring) and, hence, planar structures and, consequently, radical cations begin to dominate.<sup>47</sup> And as an extreme case, in *ortho*-salicylate a strong hydrogen bonding between the phenol hydrogen and the carbonyl group prevents the bending motion completely and, therefore, only metastable radical cations are found.<sup>46</sup> So, from the experimental point of view the background of the unusual product distribution seems convincingly confirmed.

As a further point, the behavior of thiophenols and selenol should be noted. In both cases, the rotation around the Ar- $\curvearrowright$ -XH axis is practically unhindered, as concluded from the low activation energy of  $\ll 15$  kJ mol<sup>-1</sup>. The heavy heteroatoms, however, appear to prefer an accommodation in the perpendicular structure that, as indicated before, facilitates deprotonation. Accordingly, the rapidly formed donor radical yield increasingly dominates. For Ar- $\curvearrowright$ -SeH this fraction amounts to, in fact, 90%; i.e., the structurally more stable and, therefore, dominating configuration is clearly the perpendicular one. Nevertheless, from the qualitative point of view the reaction scheme is quite analogous to that shown in equations 7a,b.

As a provisional conclusion for the described liquid-state experiments, it can be stated that a relationship has been established between the rotational mobility of the hetero substituents of the arenes and the product distribution of FET. The less restricted the rotation, bending, etc. motion is, the more apparent becomes the two product situation (parallel formation of metastable donor radical cations and corresponding deprotonated radicals).

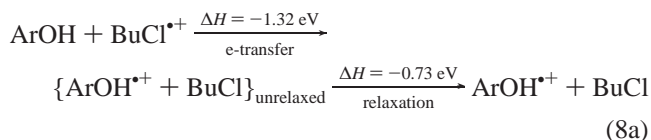
Further support for our hypothesis is provided by temperature effects, specifically by the results of matrix isolation experiments with  $\gamma$ -irradiated alkane glasses containing electron donors (e.g., phenols) at very low temperature.<sup>18,48</sup> Under those conditions, only donor radical cations have been found, as specifically reported for the particular case of a sterically hindered phenol.<sup>49,50</sup> At low temperatures the molecular dynamics and the molecule mobility are frozen. The effect can be explained by an increase of the activation barrier of the corresponding motion, and hence, the amplitude of this motion is restricted. Unfortunately, for technical reasons of our equipment, pulse radiolysis experiments, which could provide more insight, could not be performed at temperatures  $\leq -30$  °C.

#### 4. Dissociation of the Weak O–H Bond in the Perpendicular Phenol Radical Cations

In the following we will have a closer look at the energetics involved in FET in general and in particular in the rapid deprotonation (dissociation) of the unstable conformer radical cation (reaction 7b), immediately after the electron jump to the parent ion.

Overall, the *electron transfer* from the neutral ground-state phenol (ArOH) to the solvent radical cation (BuCl<sup>•+</sup>) is energetically favored by 2.05 eV. Now an energetic analysis of

the individual reaction steps should be made where the reaction is formulated in the common way (resonant molecule ArOH).

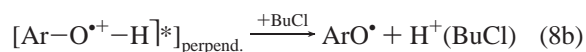


The electron transfer occurs between two electronically relaxed reaction partners. After electron jump both products, namely ArOH<sup>•+</sup> and the solvent molecule (BuCl), are primarily in an unrelaxed state, due to the change of electronic configuration within the same molecular structure.<sup>51</sup> This first step is exergonic by 1.32 eV. It follows a rapid relaxation via adjustment of the molecular geometry to the new electron distribution. The relaxation (reorganization) energy of about 0.73 eV is distributed between ArOH<sup>•+</sup> (0.19 eV) and BuCl (0.53 eV).

Certainly, before reaching the thermal equilibrium, the excess energy of the electron transfer ( $\Delta H = 1.32$  eV) is partitioned off the reactants. Considering the proton dissociation energy of about 8.7 eV in the gas phase and 2.6 eV in the liquid state (BuCl as proton acceptor), the excess energy is far from being enough for achieving deprotonation in the planar state of the phenol radical cation. Because of the strong electron-vibration coupling, the excess electronic energy is accepted by the nearest vibrations, first by the C–H valence vibrations ( $\sim 3200$  cm<sup>-1</sup> = 0.39 eV), and will be dissipated by interaction with the surroundings.

However, the additional destabilization of the deformed (twisted) donor radical cations (see reaction 7a,b), helps to overcome easily the dissociation barrier; cf. also Figure 6. This is consistent also with the observed independence of the ratio between radical cations and radicals on the type of the nonpolar solvent used. Here the free energy varies between 1 and 2 eV. Furthermore, it should be mentioned again that in the case of restricted rotation of the hetero group the prompt dissociation did not take place.

Any deprotonation in the sense of self-dissociation is energetically unfavorable. Therefore, for a mechanistic explanation of the prompt deprotonation within FET we have to take into account the solvent as proton acceptor and stabilizer, reaction 8b.



The fact that the proton affinity of many solvents, such as butyl chloride, lies just between those of the metastable planar radical cation structure and of the twisted unstable one (see Figure 5) fully corroborates our view.

A decay of the perpendicular radical cation via deprotonation, which is driven by Cl<sup>-</sup> as the nucleophile, is excluded because of the low concentration of chloride ions in the early stages. But Cl<sup>-</sup> seems to be the main carrier for the delayed and time-resolved decay of the planar ArOH<sup>•+</sup>, reaction 7c.

A potential energy diagram concerning the energetics of the solvent driven deprotonation (8b) of the dissociative cations is displayed in Figure 5. The ground state (singlet) potential is rather flat and shows the energy changes during the rotation of the Ar- $\curvearrowright$ -OH group, which amounts to  $< 15$  kJ mol<sup>-1</sup>. After ionization, the potential of the radical cation [Ar- $\curvearrowright$ -OH]<sup>•+</sup> becomes considerably deeper and the rotational motion is hindered by an activation barrier of  $\approx 60$  kJ mol<sup>-1</sup>.

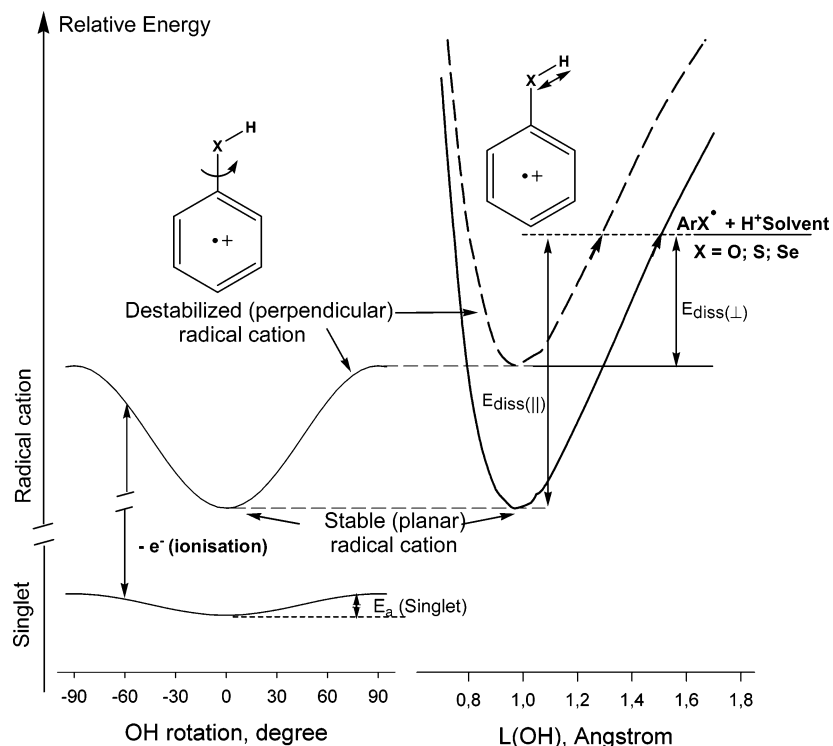


**Figure 5.** Potential diagrams describing the energetic situation of the donor molecule ( $\text{ArXH}$ ,  $\text{X} = \text{O}, \text{S}, \text{Se}$ ) in the ground state and for the different conformer radical cations. The left part shows the potentials dependent on the rotation angle, and the right part demonstrates energy changes dependent on the bond length ( $L$ ) of  $\text{Ar-XH}$ .

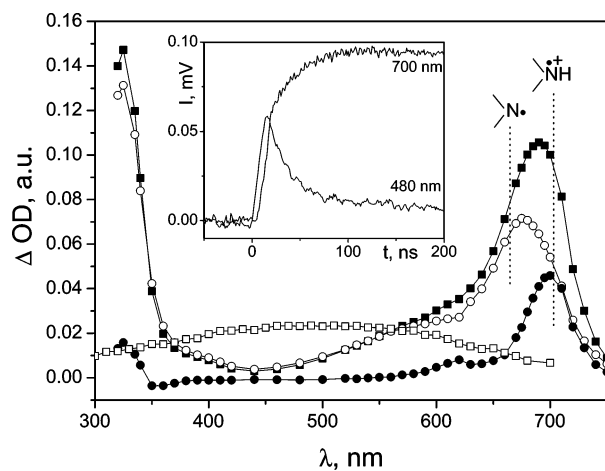


**Figure 6.** Transient spectrum obtained in the pulse radiolysis of  $10^{-3}$  mol  $\text{dm}^{-3}$  diphenylamine in deaerated *n*-butyl chloride, taken (■) 40 ns and (○) 1.2  $\mu\text{s}$  after the electron pulse. (●) represents the spectrum of the amine radical cation taken as a difference of the above spectra. For comparison, the spectrum of the  $\text{BuCl}$  radical cation is shown (□). Inset: time profiles of the same sample taken at 480 (decay of  $\text{BuCl}^{\cdot+}$ ) and 700 (formation of amine transients) nm.

The planar radical cation is metastable and is placed on the bottom of the vibration potential (Figure 5, right-hand side). The perpendicular radical cation state, however, has a much higher energy. At distances  $L > 1.3$  Å the potential of the latter crosses the level of the proton affinity of the solvent.<sup>52</sup> This critical length is easily reached during the first vibration motion and, as a consequence, dissociation (deprotonation) takes place.

### 5. Quantum-Chemical Treatment of the Dynamic Effect

Although results of quantum-chemical calculations have already been used for rationalizing the experimentally observed unusual product distribution in the FET of phenols, it seems

appropriate to present here in brief some more details of the theoretical foundation, and the quantitative as well as general conclusions derived therefrom.

The information of interest concerns, in particular,

- the dynamic behavior of the donor molecules (frequencies of vibration and bending motions),
- the electron distribution in the affected orbitals and consequences for its ionization, and
- the detailed mechanism of the dissociation of the unstable donor radical cations as far as this is a reflection of the energetics of the reaction and of some structural details (changes in bond lengths etc.).

All these data have been obtained by DFT calculations.<sup>53–55</sup>

In addition to the data used for the explanation of the experiments (see Table 1) a thorough analysis of the structure and the dynamic behavior of the phenol type compounds has been performed.<sup>56,57</sup> From that and the characterization of several tens of chalcogenol radical cations, the reaction pattern of the free electron transfer proves to follow a general mechanism:

•Donor radical cations are generated by FET (5) from a neutral compound to the solvent parent ion; i.e., an electron is removed from the HOMO of the donor. Accordingly, the structural and electronic properties of the neutral (ground state) molecules should define the properties and reactivity of the formed radical cation.

•On the femtosecond time scale, the oscillations of the phenol (donor)-type molecules result in a *continuous change of the molecular structure* by vibration, deformation, rotation, etc. motions.<sup>58</sup> Especially bending and rotational motions around the  $\text{Ar-XH}$  axis (where  $\text{X} = \text{O}, \text{S}, \text{Se}, \text{N}$ ) cause maximal changes of the molecular geometry. As can be seen in Table 1, the valence  $\text{X-H}$  vibrations are at least 10 times faster than the rotation, bending or wagging of the  $\text{Ar-XH}$  group.

However, both of them are slow in comparison to the time of the electron (transfer) jump.

- Rotation and bending motions with small activation energies (see Table 1), lead to dramatically *large changes of the electron distribution*, especially of the n-electrons of the heteroatom (cf. Figure 1 for thiophenol).

- Within the Born–Oppenheimer approximation the molecular geometry remains stiff during the period required for electron relaxation and the very fast electron-transfer jump. In all studied cases the change of the electron distribution in dependence on the angle of rotation shows a similar trend (see Figures 1 and 7). The heteroatoms carry lone electron pairs and, therefore, are potential electron donors. In the planar structure, due to the strong resonance with the  $\pi$ -electron of the aromatic ring, the n-electrons are shifted from the heteroatom to the aromatic moiety. Hence, the (HOMO) molecular orbital in the planar structure is strongly delocalized over the whole molecule. Rotation around the Ar–XH axis disturbs this coupling between ring and lone pair electrons. Therefore, the molecular orbital in the perpendicular structure assumes n-symmetry and is almost entirely localized at the heteroatom.

- The consequences emerging from all the above show up in the initial products of the FET involving the two borderline conformer structures, namely, the planar and the perpendicular (twisted) ones.

## 6. Generalization of the Influence of Bending Oscillations on the Product Distribution in FET

Described and proven in detail for phenols (cf. section 3), the hypothesis of the influence of short-lived conformers on the product pattern in FET, as it is governed by bending modes of a substituent, should hold and, therefore, be considered also for other chemical structures. As for a model, molecules consisting of an aromatic ring and a marked substituent come to mind. The term *marked substituent* in this context refers to a group that is able to easily undergo any bending motions relative to the aromatic ring. The following aspects and, relative to the phenol-type systems, now more generalized statements deserve particular attention.

If the substituent contains heteroatoms that contribute to the polarization of the molecule, then any of their motions will be reflected in the fluctuation of the electron density in the molecule. The continuous bending of the substituent in this dynamic situation is coupled to a corresponding change of molecular conformations, which thus means it continuously passes through a diversity of states with different electron density distributions, as a function of the angle of twist.

The fluctuation of the (HOMO) electrons may be directed from the n-orbital to the aromatic ring (phenols) or from a ring  $\pi$ -orbital to the heterosubstituent (benzylsilanes; see below).

For detecting and identifying the phenomenon of conformer-dependent product formation, a possibility of differentiating the products should exist. In the case of a rigid molecule structure (skeleton), radical cations derived from the different conformers, unfortunately, isomerize rapidly to the energetically stable state and, consequently, there is no chance for observing the effect.

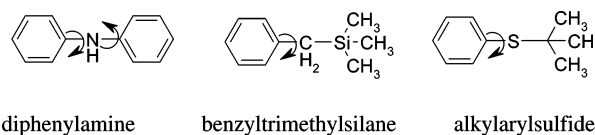
But in the case where the product radical cation of one conformer is (meta)stable and that of the other one is dissociative, like in the case of phenols, two different products should appear simultaneously on the time scale of the electron-transfer overall reaction.

Furthermore, because the observation of the products is limited to the time scale  $\geq 10$  ns, i.e., the time range where the

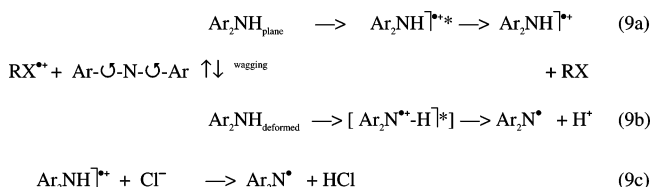
diffusion-controlled overall reaction 6 takes place, the dissociation of the unstable conformer cation must be faster than this time limit. The *detection method* by real time spectroscopy thus deals again with a *steady state situation*. It should specifically be recognized though that the nanosecond technique discriminates any other transient processes that may take place at longer times after a pulse of radiolysis.<sup>59</sup>

## 7. Further Experimental Examples of FET

Having these points, the search for further experimental examples was focused on substances with similarly *good leaving groups* as the proton (cf. phenols) or other low-energetic ions. Indeed, primary and secondary aromatic amines, benzyltrimethylsilanes and highly substituted aromatic sulfides appear to fall into this category. Structural formulas with rotating arrow indicating characteristic bending motions:



**Diphenylamine and Anilines.** Figure 6 presents optical absorption spectra taken in the pulse radiolysis of diphenylamine dissolved in *n*-butyl chloride.<sup>60</sup> Although the spectra of the FET products strongly overlap, a spectral and kinetic analysis nevertheless revealed unambiguously that amine radical cations as well as aminyl radicals were formed synchronously. The time profiles given as inset of Figure 6 show the FET reaction (9a,b)



from the educt (solvent radical cation at 480 nm) as well as the product side (amine transients at 700 nm). The amine radical cation and a considerable fraction of the aminyl radical are formed instantly (cf. also reactions 9a,b). This can be also seen for the profiles taken for longer times, cf. Figure 8.

Taking into account an asymmetric wagging motion involving both Ar–N–Ar bonds, the deformation leads to changes of structure from planar (0°) to perpendicular (90°), which results in a considerable shift of the electron distribution toward the heteroatom. This is shown in Figure 7.

For a quantitative description of the reaction channels (9a,b,c) we simulated time profiles at certain characteristic wavelengths where the overall optical absorptions are superimpositions of the individual absorptions of all involved species but contribute to different extents. This is shown in Figure 8. The best fit of the aminyl radical absorption traces (□) has been achieved for a ratio of 50:50 between the two possible reaction channels. This convincingly confirms the applied underlying mechanistic scheme.

We assume that, in this system, it is the wagging motion that is responsible for the formation of the two instant products of reaction (9a,b). As indicated in the formulas, the metastable mesomer radical cation is that with delocalized charge (9a) whereas in the other one the charge is concentrated mainly on the nitrogen atom (9b). This picture is based on an analogous simplification as was made for phenols. In reality, a diversity



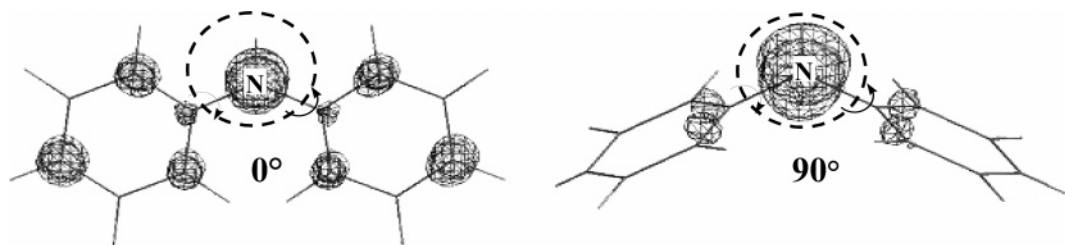


**Figure 7.** Electron distribution of the HOMO electrons of DPA given for the planar ( $0^\circ$ ) and the twisted state ( $90^\circ$ ).

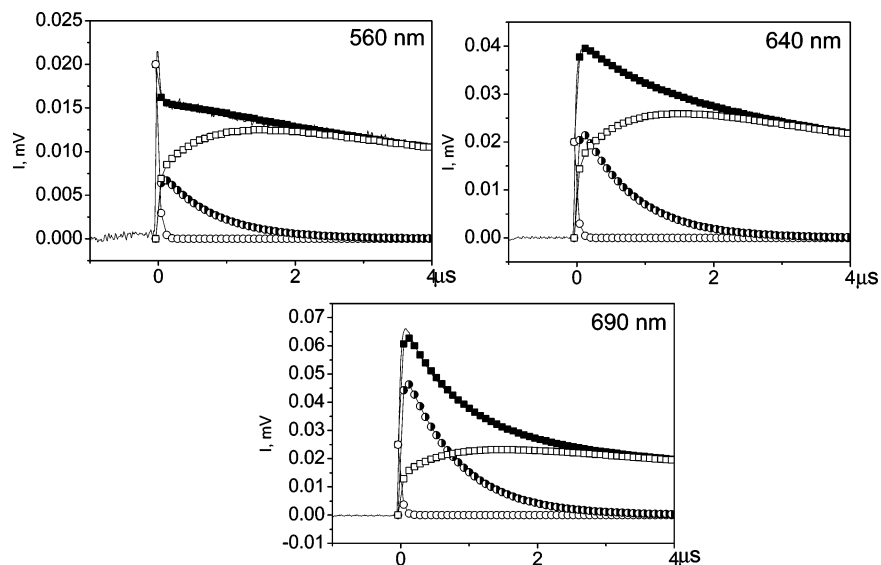


**Figure 8.** Time profiles showing the correlation between kinetic simulation and experimental data: (—) experimental profile. Simulated time profiles: (■) sum profile, (○) chlorobutane radical cation, (●) DPA radical cation  $\text{Ar}_2\text{NH}^{\bullet+}$ , (□) DPA radical  $\text{Ar}_2\text{N}^\bullet$ .

of more or less deformed states exists during the wagging oscillation at any individual moment.

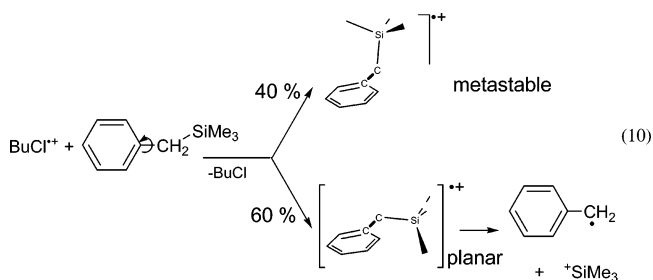
Although amine radical cations are known to be nearly persistent, in the special case of charge localization on the N atom the species seems to be dissociative; i.e., it deprotonates rapidly. This has, indeed, been observed in the experiment and is also supported by the results of quantum-chemical calculations. A collection of corresponding data is given in Table 2. Except for stable tertiary structures such as in triphenylamine or dimethylaniline,<sup>41</sup> all the primary and secondary aromatic amines follow the same reaction pattern as reported for diphenylamine. Interestingly, for photosensitized radical cations derived from slightly deformed secondary aromatic amines, a rapid unimolecular deprotonation with  $k \approx 10^8 \text{ s}^{-1}$  has been reported.<sup>61</sup> This nicely corroborates our hypothesis of the rapid deprotonation of the twisted solute cations described in this paper.

As an exception, FET involving secondary aromatic amines with rigid structures exclusively yielded amine radical cations (acridane, carbazole<sup>62</sup>). In contrast, the more mobile phenothiazine structure gives both FET products; see Table 2. These findings are also consistent with the hypothesis concerning the reflection of the molecular motions in FET.

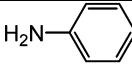
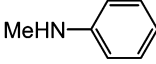
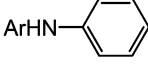
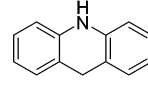
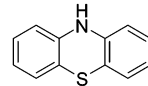
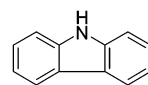
**Benzyltrimethylsilanes.** These compounds also contain a substituent that can be bent against the aromatic ring. The favored leaving group should in this case be the trimethylsilyl cation. Although the molecular structure differs from the former examples (phenols, aromatic amines), the FET with benzyltrimethylsilanes principally follows the same reaction pattern, as displayed in eq 10. The rotating substituent causes electron fluctuation in the HOMO, which, in this case, involves  $\pi$ -electrons. Two distinguishable product radical cations are,

indeed, formed in the electron transfer of which one is dissociative and the other one is metastable, as experimentally observed in pulse radiolysis experiments (see Figure 9). Because of the inverse electron shift ( $\pi$  electrons from the ring instead of  $n$ -electrons as for, e.g., phenols) the stability of the cation conformers changed: the planar conformer is dissociative whereas the deformed one is metastable. Hence, part of the dissociative product (60%) is formed rapidly, whereas the remaining 40% are generated in a delayed manner.<sup>63–65</sup>

Figure 10 shows transient absorption spectra obtained in the pulse radiolysis of benzyltrimethylsilane in  $\text{N}_2$ -purged *n*-butyl chloride solution. The main absorption is due to the corresponding metastable radical cation ( $\lambda = 330, 550 \text{ nm}$ ).<sup>64</sup> The long-lasting absorption in the UV, however, is caused by the benzyl radicals, which show a characteristic maximum in this wavelength range. The kinetic situation becomes clearer by looking at the corresponding time profiles in Figure 10. With the decay of the solvent radical cation (640 nm), both the metastable silane radical cation (530, 310 nm) and the benzyl radical as the observable direct successor of the dissociative silane species (fast part of the profile taken at 260 nm) are seen to be present



**TABLE 2: Calculated Times of One Motion of Bending (Torsion, Wagging) ( $t_{\text{bending}}$ ) and Valence (Stretching) ( $t_{\text{valence}}$ ) Oscillations (B3LYP/6-31G(d), Scale Factor  $f = 0.96$ )<sup>a</sup>**

	$t_{\text{bending}}$ [ $10^{-15}$ s]	$t_{\text{valence}}$ [ $10^{-15}$ s]	$E_a$ singlet (cation) [kJ mol <sup>-1</sup> ]	estimated product ratio (•+)/(•)	remarks	ref.
	59.1	9.1	23 (150)	50:50	torsion	60
	334	9.3	25 (112)	50:50	torsion	60
	608	9.2	13	50:50	DPA: torsion	60
	760	9.1	1.3 (19)	85:15	acridane, slightly wagging	62
	610	9.2	7.4 (24)	50:50	phenothiazin wagging	62
	-	9.1	-	100:0	carbazol, rigid skeleton	62

<sup>a</sup>  $E_a$  is the energy barrier for rotation along the Ar–N– axis or bending motions for the singlet ground state, as well as for the radical cation (in brackets).

simultaneously. The delayed dissociation of the metastable silane cation is reflected by the delayed part of the benzyl radical absorption (Figure 10, 260 nm).

This behavior has been observed for a variety of differently substituted silanes and can thus be generalized.<sup>64</sup> Corresponding data are given in Table 3. In the case of cyclic substituents (fluorenyl and xanthenyl trimethylsilanes<sup>65</sup>) a convincing relationship can be established with the flexibility of the silane substituent, which, in turn, may allow a calibration of the ratio between rapidly formed radicals and metastable radical cations. This correlation is, in fact, one of the main arguments supporting the hypothesis that the products of the free electron transfer are a direct reflection of the molecular dynamics. The examples with benzyl trimethylsilane type compounds clearly manifest

the generality of the FET concept. The rapid dissociation of the unstable primary radical cation happens also if instead of protons other leaving energetically favored groups are applied. In the case of the above-mentioned silane compounds the leaving entity is the trimethylsilyl cation.

A further experimental example is the FET-induced oxidation of phenyl benzyl sulfides for which the dissociative ionic products are two couples such as arylmethyl radicals/sulfur-centered cations and trityl cations/thiyl radicals.<sup>66</sup> Here by energetic reasons a split but also specific dissociation pattern of the unstable radical cation seems to exist. This matter is just under investigation.

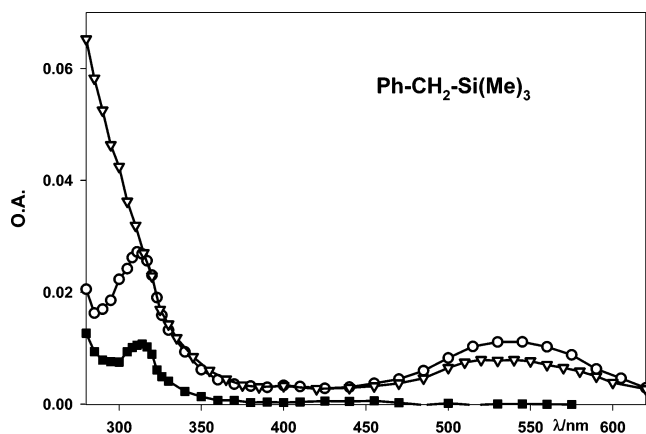


**Figure 9.** Transient absorption spectra taken in the pulse radiolysis of a  $1.1 \times 10^{-3}$  mol dm<sup>-3</sup> solution of benzyltrimethylsilane in *n*-butyl chloride, purged with N<sub>2</sub> (100 ns (○) and 2 μs (■) after the pulse) and in O<sub>2</sub> saturated solution (after 100 ns (▽)). Here the strong UV absorption is caused by butylperoxyl radicals.

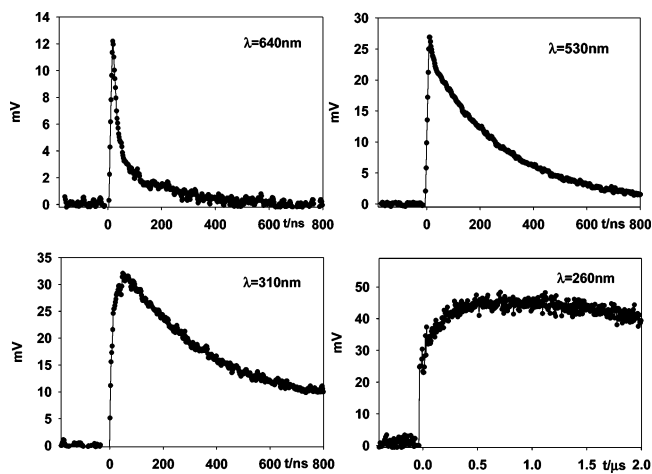


**Figure 10.** Time profiles of the  $n\text{-C}_4\text{H}_9\text{Cl}^+$  (640 nm), the silane radical cation (530, 310 nm) and the fragment radical (long-time contribution at 310 nm, main part at 260 nm) taken in the pulse radiolysis of a  $2 \times 10^{-3}$  mol dm<sup>-3</sup> solution of benzyltrimethylsilane in *n*-butyl chloride purged with nitrogen.

**TABLE 3: Calculated Times of One Motion of Torsion (Wagging) and Valence (Stretching) ( $\nu_{\text{valence}}$ ) Oscillations (B3LYP/6-31G(d), Scale Factor  $f = 0.96^a$ )**

	$t_{\text{rot,def}}$ [ $10^{-15}$ s]	$t_{\text{valence}}$ [ $10^{-15}$ s]	$E_a(\text{S})$ , singlet (cation), kJ mol <sup>-1</sup>	product ratio (•+)/(•)	remarks	ref.
	850	55	5 (39)	70:30	non yet published	66
$R_3\text{-Ar-CR}_1\text{R}_2\text{-SiMe}_3$ 	1330-2380	37	14-24 (57-87)	40:60	$R_{1,2} = \text{H, Me, Ph};$ $R_3 = \text{H, PHCO-};$ 10 compounds	64
	600	40	-	25:75	xanthenyl $R = \text{Me, Ph};$ 6 examples	65
	-	40	-	100:0	fluorenyl $R = \text{Me, Ph};$ 2 examples	65

<sup>a</sup>  $E_a(\text{S})$  denotes the energy barrier of rotation along the Ar-X (where X = O, S, N and C) axis and bending motions for the singlet ground state, as well as for the radical cation (in brackets).

## 8. Time Regime of the Components of FET Related to Basic (Physical) Relaxation Phenomena

At this point it is deemed appropriate to accommodate, for comparison, all the events around FET into a general time scale. Figure 11 shows a time axis ranging from atto- to microseconds.<sup>68</sup> Above the scale, defined time domains are associated with individual processes, such as electron fluctuations in organic molecules, molecular oscillation (motions) and diffusion-controlled bimolecular events. Below the time axis, the different steps of the FET are arranged.

The diffusion-controlled overall (gross) reaction is conditioned by the transport process and, accordingly, needs nanoseconds. This, in turn, limits the experimental detection to this time range. Splitting FET into individual steps, the electron jump from the donor to the parent solvent radical cation is the fastest one, completed within less than a few femtoseconds, possibly just hundreds of attoseconds. The intramolecular dynamic motions

need longer times (femtosecond scale), and vibrations exhibit at least 10 times higher frequencies than rotation and bending motions. Vibrational relaxation is likely to be a bit slower than vibrational motions, which would be in line with our assumption that the dissociation is the dominating process in the decay of the perpendicular radical cation, reaction 7b. In other words, after the electron jump takes place, the dissociation should happen during the first vibration of the relevant bond.

The processes taking place in the nanosecond time domain, such as the diffusion-controlled gross process (6) and also the delayed dissociation of the metastable donor radical cations (7c), can directly be observed by time-resolved spectroscopy in pulse radiolysis experiments. Transient absorption spectra (see figures throughout this paper) enable the identification of the FET products, and the time profiles provide kinetic and yield information. For the latter case, the observation of a rapid (reaction 7b) and a delayed part (reaction sequence 7a,c) of the final radical products can clearly be distinguished. This gives direct access to the determination of the respective yields of the competing processes (7a,b), i.e., to the quantification of both channels in the electron transfer, forming unstable and metastable donor radical cations. A typical example has been given in Figure 8.

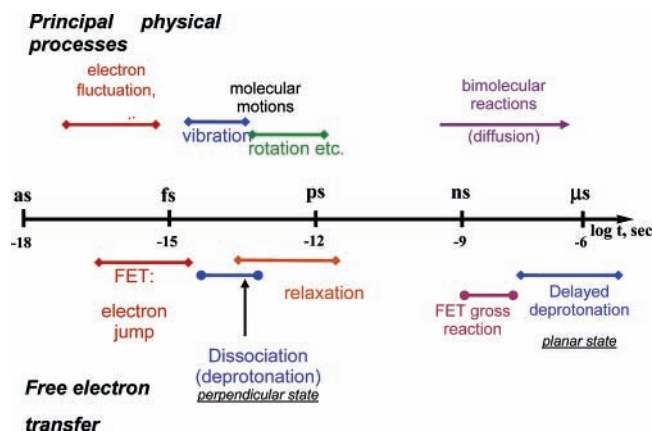


**Figure 11.** Time range of processes relevant in free electron transfer (FET). (×) rotation (torsion) stands also for other similar motions such as necking, wagging, bending, etc.

## 9. Quantification of the Dynamic Effect in FET

From the qualitative point of view, the influence of molecular dynamics on the free electron transfer seems to be well established on the basis of the data presented here. Now, the question of the quantification arises. The main problem lies in the exact evaluation of the relationship between the intramolecular deformation motions of the substituents and the experimentally determined product distribution.

The intramolecular motions that are connected with an efficient electron fluctuation of the reaction-concerned orbital ( $n$  or  $\pi$ ) are complex and require, in principle, a complete

description of all involved rotation, torsion, bending, wagging, etc., modes. The single modes can be determined by quantum chemical calculations (see Tables 1–3). These data provide an estimate for the time range of the oscillations but also how this is related to the time of the electron jump within the FET. Indeed, the calculations unambiguously confirm that the electron jump is faster than the oscillations by at least two orders in magnitude.

The interpretation of the two ionization pathways (formation of stable and dissociative donor radical cations) is made, as mentioned before, with the simplification that the oscillation-conditioned diversity of conformers is reduced to two limiting states, the planar molecule and the perpendicular structure. The crucial point here is the definition of the border angle separating these two prototypes. Unfortunately, because of the nonharmonic motions and their superimpositions, this problem is still too complex to be solved in a satisfactorily manner through computational calculations.

Including the dielectric continuum (influence of solvent) in the DFT calculations, only a minor influence has been found on the oscillation data. We further checked on the effect of the surrounding solvent as a homogeneous heat bath by simple molecular dynamics calculations. A statistic evaluation of the deformation of the substituent against the aromatic ring of the donor resulted in values around  $10^\circ$  (at room temperature) for the critical angle. This differs significantly from the deformation angle of  $45^\circ$  adopted as a borderline between the two conformer categories. The experimental results can, therefore, not be explained on the basis of the influence of the solvent surroundings. That means also that the solvent has no marked effect on any of the DFT data (frequencies) calculated under vacuo.

A complete picture should finally include a detailed description of the kinetics involved in the FET phenomenon. Because this is all based on known kinetic models, this treatment will be presented in a following publication,<sup>66</sup> which will state that the rapid change of the conformer states (high frequency of oscillation) results, indeed, in the two-channel model and, therefore, satisfactorily explains the two-product situation in free electron transfer.

## 10. Summary

The free (i.e., unrestricted) electron transfer (FET) from donor molecules to solvent parent radical cations of alkanes and alkyl chlorides is a well-known reaction type, conveniently studied by means of electron pulse radiolysis. In the presence of arenes with heteroatom-centered substituents, such as phenols, aromatic amines, benzylsilanes, etc., as electron donors, this electron transfer interestingly leads to the practically simultaneous formation of two distinguishable ionization products, namely, donor radical cations and fragment radicals, in comparable amounts.

This unusual behavior is interpreted as a reflection of the femtosecond dynamics of the donor molecules and an extremely rapid electron jump within the FET. Because this jump is much faster than the rotation and bending motions of the substituents, the donor presents itself as a dynamic mixture of conformers. The crucial point is that, concomitant with these motions, the HOMO and n-electrons continuously fluctuate in these conformers, which causes extremely different electron distributions in the respective singlet ground states. Ionization of this dynamic conformer mixture results in the formation of two types of radical cations, one of which is metastable whereas the other one dissociates immediately into radicals and cations.

Two general aspects of the free electron transfer should be stressed, namely:

(i) The existence of the seemingly paradoxical phenomenon that a diffusion-controlled electron-transfer reaction is governed (from the point of view of the products) by femtosecond molecule dynamics. Analysis of the overall electron-transfer reaction in terms of its individual steps reveals that, mechanistically, the rapid electron jump ( $\leq 1$  fs) is the deciding one.

(ii) The ultrafast FET from donors to  $\sigma$ -type (saturated) radical cations differs completely from the common electron-transfer concepts, which pertains to the electron transfer in nonpolar media as well as to the special phenomenon of the influence of femtodynamics on the product cation formation.

**Acknowledgment.** We cordially thank Prof. Klaus-Dieter Asmus (Berlin), Drs. Ralf Hermann and Wolfgang Naumann for many discussions and helpful proposals. Furthermore, we thank all young co-workers which enthusiastically took part in the investigations.

**Supporting Information Available:** A formal analysis of the free electron-transfer kinetics. This material is available free of charge via the Internet at <http://pubs.acs.org>.

## References and Notes

- (1) Strehlow, H. *Rapid Reactions in Solution*; VCH Verlag: Weinheim, New York, Basel, Cambridge, 1992; p 249.
- (2) Connors, K. A. *Chemical Kinetics. The Study of Reaction Rates in Solution*; VCH Publishers: New York, Weinheim, Cambridge, 1990; pp 13 (diff), 209.
- (3) Martin, M. M.; Hynes, J. T. *Femtochemistry and Femtobiology, Ultrafast Events in Molecular Science*; Elsevier: Amsterdam, 2004.
- (4) Zewail, A. H. In *Femtochemistry*; De Schryver, F. C., De Feyter, S., Schweitzer, G., Eds.; Wiley-VCH: Weinheim, New York, 2001; p 9.
- (5) Zewail, A. H. In *Femtosecond Chemistry I*; Manz, J., Wöste, L., Eds.; VCH-Verlag: Weinheim, 1995; p 18.
- (6) Atkins, P. W. *Physikalische Chemie*; VCH: Weinheim, 1990; p 475.
- (7) Levin, R. D.; Bernstein, R. B. *Molekulare Reaktionsdynamik*; Teubner: Stuttgart, 1991; p 56.
- (8) Nibbering, E. T. J.; Elsaesser, T. *Chem. Rev.* **2004**, *104*, 1887.
- (9) Reinhold, J. *Quantentheorie der Moleküle*; Teubner: Stuttgart, 1994; p 119.
- (10) Lin, C. L.; Swalen, J. D. *Rev. Mod. Phys.* **1959**, *31*, 841.
- (11) Brede, O.; Hermann, R.; Naumann, W.; Naumov, S. *J. Phys. Chem. A* **2002**, *106*, 1398.
- (12) Brede, O. *Res. Chem. Intermed.* **2001**, 27709.
- (13) Brede, O.; Hermann, R.; Naumov, S.; Zarkadis, A. K.; Perdikomatis, G. P.; Siskos, M. G. *Phys. Chem. Chem. Phys.* **2004**, *6*, 2267.
- (14) Brede, O.; Ganapathi, M. R.; Naumov, S.; Naumann, W.; Hermann, R. *J. Phys. Chem. A* **2001**, *105*, 3757.
- (15) Mahalaxmi, G. R.; Hermann, R.; Naumov, S.; Brede, O. *Phys. Chem. Chem. Phys.* **2000**, *2*, 4947.
- (16) Brede, O.; Mehnert, R.; Naumann, W. *Chem. Phys.* **1987**, *115*, 279.
- (17) Sander, M. V.; Brummund, V.; Luther, K.; Troe, J. *J. Phys. Chem.* **1993**, *97*, 8378.
- (18) Hamill, W. H. In *Radical Ions*; Kaiser, E. T., Kevan, L., Eds.; Interscience: New York, 1968; p 321.
- (19) Stienlet, D.; Ceulemans, J. *J. Phys. Chem.* **1992**, *96*, 8751 and citations herein.
- (20) Luyckx, G.; Ceulemans, J. *J. Chem. Soc., Faraday Trans.* **1991**, *87*, 3499.
- (21) Toriyama, K. In *Radical Ionic Systems – Properties in condensed Phases*; Lund, A., Shiotani, M., Eds.; Kluwer Academic Publishers: Dordrecht, The Netherlands, 1991; p 99.
- (22) Lindgren, M.; Shiotani, M. In *Radical Ionic Systems – Properties in condensed Phases*; Lund, A., Shiotani, M., Eds.; Kluwer Academic Publishers: Dordrecht, The Netherlands, 1991; p 125.
- (23) Mehnert, R.; Brede, O.; Bös, J. *Z. Chem. (Leipzig)* **1977**, *17*, 268.
- (24) Mehnert, R. In *Radical Ionic Systems – Properties in condensed Phases*; Lund, A., Shiotani, M., Eds.; Kluwer Academic Publishers: Dordrecht, The Netherlands, 1991; p 231.
- (25) Mehnert, R.; Brede, O.; Naumann, W. *Ber. Bunsen-Ges. Phys. Chem.* **1984**, *88*, 71.
- (26) Mehnert, R.; Brede, O.; Naumann, W. *Ber. Bunsen-Ges. Phys. Chem.* **1982**, *86*, 525 and recent measurements.
- (27) *Handbook of Chemistry and Physics*, 73rd ed.; Lide, D. R., Ed.; CRC Press: Boca Raton, FL, 1992; pp 10–214.

- (28) Rehm, D.; Weller, A. *Ber. Bunsen-Ges. Phys. Chem.* **1969**, *73*, 834.
- (29) Kavarnos, G. J. *Fundamentals of Photoinduced Electron Transfer*; VCH Publishers: New York, 1993; p 53.
- (30) Brede, O.; Mehnert, R.; Naumann, W.; Cserep, Gy. *Radiat. Phys. Chem.* **1982**, *20*, 155.
- (31) Arai, S.; Kira, A.; Imamura, M. *J. Phys. Chem.* **1976**, *80*, 1968.
- (32) Trifunac, A. D.; Sauer, M. C.; Shrob, I. A.; Werst, D. W. *Acta Chem. Scand.* **1997**, *51*, 158 (Review).
- (33) de Haas, M. P.; Hummel, A.; Infelta, P. P.; Warman, J. M. *Can. J. Chem.* **1977**, *55*, 2249.
- (34) Zador, E.; Warman, J. M.; Hummel, A. *Chem. Phys. Lett.* **1973**, *23*, 363.
- (35) Brede, O.; Helmstreit, W.; Mehnert, R. *Chem. Phys. Lett.* **1974**, *316*, 402.
- (36) Turro, N. J. *Modern Molecular Photochemistry*; University Science Books: Mill Valley, CA, 1991; p 6.
- (37) Kavarnos, G. J. *Fundamentals of Photoinduced Electron Transfer*; VCH Publishers: New York, 1993; p 103.
- (38) Levine, R. D.; Bernstein, R. B. *Molekulare Reaktionsdynamik*; B. G. Teubner: Stuttgart, 1991; p 44.
- (39) Fartahaziz, M. A.; Rodgers, J. *Radiation Chemistry, Principles and Applications*; VCH Publishers: Weinheim, 1987.
- (40) Mohan, H.; Hermann, R.; Naumov, S.; Mittal, J. P.; Brede, O. *J. Phys. Chem. A* **1998**, *102*, 5754.
- (41) Brede, O.; Kapoor, S.; Mukherjee, T.; Hermann, R.; Naumov, S. *Phys. Chem. Chem. Phys.* **2002**, *4*, 5096.
- (42) Brown, W.; Herron, J. T.; Kahaner, D. K. *Int. J. Chem. Kinet.* **1998**, *20*, 51.
- (43) Hermann, R.; Dey, G. R.; Naumov, S.; Brede, O. *Phys. Chem. Chem. Phys.* **2000**, *2*, 1213.
- (44) Brede, O.; Hermann, R.; Naumov, S.; Mahal, S. *Chem. Phys. Lett.* **2001**, *350*, 165.
- (45) Dey, G. R.; Hermann, R.; Naumov, S.; Brede, O. *Chem. Phys. Lett.* **1999**, *310*, 137.
- (46) Brede, O.; Hermann, R.; Karakostas, N.; Naumov, S. *Phys. Chem. Chem. Phys.* **2004**, *6*, 5184.
- (47) Joshi, R.; Naumov, S.; Kapoor, S.; Mukherjee, T.; Hermann, R.; Brede, O. *J. Phys. Org. Chem.* **2004**, *17*, 665.
- (48) Shida, T. *Electronic Absorption Spectra of Radical Ions*; Elsevier: Amsterdam, 1988; p 2.
- (49) Brede, O.; Orthner, H.; Zubarev, V.; Hermann, R. *J. Phys. Chem.* **1996**, *100*, 7097.
- (50) Zubarev, V.; Brede, O. *Acta Chem. Scand.* **1997**, *51*, 224.
- (51) Medvedev, E. S.; Oshero, V. I. *Radiationless Transitions in Polyatomic Molecules*; Springer-Verlag: Berlin, 1995; p 53.
- (52) *Energien chemischer Bindungen, Ionisationspotentiale und Elektronenaffinitäten*; Wedenejew, W. J., et al., Ed.; VEB Deutscher Verlag für Grundstoffindustrie: Leipzig, 1970; p 81.
- (53) Becke, A. D. *J. Chem. Phys.* **1993**, *98*, 5648.
- (54) Becke, A. D. *J. Chem. Phys.* **1996**, *104*, 1040.
- (55) Lee, Ch.; Yang, W.; Parr, R. G. *Phys. Rev. B* **1987**, *37*, 785.
- (56) Hermann, R.; Naumov, S.; Mahalaxmi, G. R.; Brede, O. *Chem. Phys. Lett.* **2000**, *324*, 265.
- (57) Hermann, R.; Naumov, S.; Brede, O. *J. Mol. Struct. (THEOCHEM)* **2000**, *532*, 69.
- (58) Günzler, H.; Gremlich, H.-U. *IR Spectroscopy, an Introduction*; VCH: Weinheim, 2002.
- (59) Hummel, A. In *Radiation Chemistry, Principles and Application*; Fartahaziz, Rodgers, M. A. J., Eds.; VCH Publishers: Weinheim, 1987; p 98.
- (60) Maroz, A.; Hermann, R.; Naumov, S.; Brede, O. *J. Phys. Chem. A* **2005**, *109*, 4690.
- (61) Dombrowski, G. W.; Dinnocenzo, J. P.; Zielinski, P. A.; Fraid, S.; Wosinska, Z. M.; Gould, I. R. *J. Org. Chem.* **2005**, *70*, 3791.
- (62) Brede, O.; Maroz, A.; Hermann, R.; Naumov, S. *J. Phys. Chem. A* **2005**, *109*, 8081.
- (63) Brede, O.; Hermann, R.; Naumov, S.; Perdikomatis, G. P.; Zarkadis, A. K.; Siskos, M. G. *Chem. Phys. Lett.* **2003**, *376*, 370.
- (64) Brede, O.; Hermann, R.; Naumov, S.; Perdikomatis, G. P.; Zarkadis, A. K.; Siskos, M. G. *Chem. Phys. Phys. Chem.* **2004**, *6*, 2267.
- (65) Karakostas, N.; Naumov, S.; Siskos, M. G.; Zarkadis, A. K.; Hermann, R.; Brede, O. *J. Phys. Chem.* **2005**, *109*, 11679.
- (66) Karakostas, N.; Brede, O. Not yet published.
- (67) Brede, O.; Bös, J.; Mehnert, R. *Ber. Bunsen-Ges. Phys. Chem.* **1980**, *84*, 63.
- (68) Klessinger, M.; Michl, J. *Excited States and Photochemistry of Organic Molecules*; VCH Publishers: New York, Weinheim, Cambridge, 1995.